Inductive measurements and study of the upper critical field in UBe_{13} single crystals as a function of field orientation

P. J. C. Signore, B. Andraka, G. R. Stewart,* and M. W. Meisel†
Department of Physics and Center for Ultralow Temperature Research, University of Florida, 215 Williamson Hall, P.O. Box 118440, Gainesville, Florida 32611-8440
(Received 17 March 1995; revised manuscript received 28 April 1995)

Using sensitive mutual induction techniques, we have measured the real part of the susceptibility, $\chi'(B,T)$, and the imaginary part, $\chi''(B,T)$, for three UBe_{13} single crystals below 1 K and in fields up to 8 T oriented along the [100] and [110] directions, with particular emphasis on the region near the zero-field critical temperature T_c. In this regime and within our experimental uncertainties of 0.5 mK and 5 mT, no anisotropy was observable for any of the samples. For all three samples, the magnetic susceptibility between 4 and 15 K was measured and subtle features were found for two of the samples around 10 K. For one of these specimens, an anomaly in $\chi'(B,T)$ was observed below the superconducting transition and is likely due to flux pinning mechanisms. The $B_{c2}(T)$ phase diagrams are presented and compared to the results of other workers. Finally, the temperature dependence of the penetration depth for $0.1 \leq T/T_c \leq 0.5$ was found to be close to T^3, independent of field orientation, and these data are presented and discussed.

I. INTRODUCTION

A variety of experimental results on superconducting UBe_{13} has been taken as evidence for non-BCS-like superconductivity in this heavy-fermion system.[1,2] For example, specific heat (C) measurements[3] show that below the critical temperature ($T_c \approx 890$ mK), C does not fall off exponentially but follows a power-law dependence close to T^3. Moreover, penetration-depth data[4–6] also indicate a slower temperature dependence than expected for BCS-like superconductors, and nonexponential decay of ultrasound absorption at very low temperature gives further evidence for unusual superconductivity.[7] However, the aforementioned results only offer suggestive evidence for unconventional superconductivity, where the definition of unconventional has been given explicitly by Rainer[8] and Fulde, Keller, and Zwicknagl.[9] Other experimental investigations, such as photoemission spectroscopy, Josephson-junction tunneling,[10] nonlinear Meissner effect studies,[11] and measurements of the specific heat under uniaxial stress[12] have been proposed to test the conventionality of superconductors directly.

An experiment that has been proposed as a "crucial" test for unconventionality is the measure of the anisotropy of the upper critical magnetic field, $B_{c2}(T)$, in the limit $T/T_c \rightarrow 1$.[8,13] The relationship between the angular dependence of $B_{c2}(T)$ and the symmetry of the superconducting gap parameter has been discussed in detail by Gor'kov.[13] Although $B_{c2}(T)$ of UBe_{13} has already been well studied,[14–20] the anisotropy in $B_{c2}(T)$ has only been investigated by Alekseevskii *et al.*[21] and Aliev *et al.*,[22] who measured the magnetoresistance of an unannealed UBe_{13} single crystal as a function of orientation. These authors reported a strong anisotropy of $B_{c2}(T)$ even in the limit $T/T_c \rightarrow 1$, and they suggest that their results supported the existence of lines of zeros in the superconducting gap. In the same work, normal-state thermal conductivity measurements were reported and indicated a possible magnetic transition around 8 K, which was supported by the earlier magnetostriction measurements of Kleiman *et al.*[23] However, the existence of this magnetic transition later became somewhat controversial when several groups conducting similar experiments did not observe any sign of such a transition.[24,25]

The primary motivation for our work was to study the anisotropy of $B_{c2}(T)$ in high-quality, annealed, single crystals of UBe_{13} for samples that do not exhibit any sign of magnetic ordering near 8 K and for specimens that do. We have measured the normal-state magnetic susceptibility of several UBe_{13} single crystals have been found several (one of which is called herein sample 1) devoid of any trace of a magnetic transition. Of the ten specimens whose high-temperature susceptibility was studied, only two samples (listed as 2 and 3 in this paper) showed any sign of an "anomaly" near 10 K. In fact, as will be shown below, the presence of this possible anomaly is only observable in a subtle manner. Using a sensitive mutual inductance technique, we determined $B_{c2}(T)$ for magnetic fields up to 8 T oriented parallel to the [100] and [110] directions, with particular emphasis on the region near the zero-field critical temperature. A preliminary report of our work has been published.[26] As discussed below, in the process of looking for the anisotropy of $B_{c2}(T)$, we have found a number of interesting results, such as the appearance (for sample 3) of a transition line, within the superconducting state. This line was constructed, in part, from magnetic field sweeps at constant temperature, which were motivated by the specific-heat measurements as a function of field at constant temperature by Ellman *et al.*,[27] who reported the presence of a transition line below the superconducting state. In addition, our measurements allowed us to establish the temperature dependence of the penetration depth of single

crystal UBe_{13} in zero field and to compare it to the results of other workers.[4–6]

The remainder of the paper is organized in the following manner. The details of the experimental techniques are presented in the following section, where the fabrication protocols for the samples are also described. In the third section, the results of our measurements are given. After a detailed discussion of our observations in Sec. IV, we conclude by summarizing our work.

II. EXPERIMENTAL ASPECTS

We measured $\chi'(B,T)$ and $\chi''(B,T)$ using a standard mutual inductance technique operating at either 317 or 417 Hz. The samples and the coils (excitation and pick-up) were placed at the center of a superconducting magnet, which can provide fields up to 8 T. They were mounted at the end of a copper finger, which was bolted to the mixing chamber of a dilution refrigerator. The details of our experimental configuration are given by Signore.[28]

Measurements were performed under either constant field or constant temperature conditions. The temperature was controlled with a germanium resistor mounted on the mixing chamber, which was in the low-field region. A RuO_2 resistor[29] of known magnetoresistance was mounted at the end of the cold finger to check the thermal gradient between the sample and the mixing chamber. The gradient was found to be less than 5 mK at 8 T and 100 mK.

The single crystals were obtained by slow cooling a melt of high-purity components in a BeO crucible, which contained an aluminum flux. The aluminum flux was removed with NaOH. Several batches were made; samples 1 and 2 originate from the same batch, while sample 3 comes from a different batch prepared with a different amount of aluminum and with a faster cooling rate. The samples were annealed together for six months at 1000 °C. During annealing, the crystals were placed in a BeO crucible with a separated piece of Be. The crucible, closed with a BeO lid, was cowrapped with Ta foil and hermetically sealed in a Ta tube with end caps. The ensemble was sealed in a quartz tube, which held a vacuum. Table I summarizes the pertinent characteristics of the specimens. The specimens were nearly cubic in shape,

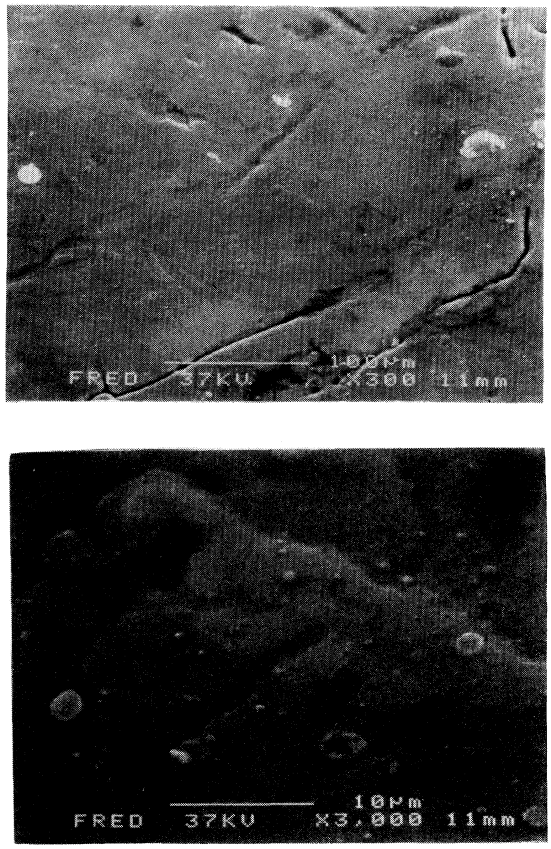

FIG. 1. SEM pictures of the surface of sample 1: (top) 100-μm scale and (bottom) 10-μm scale.

and x-ray analysis on sample 1 ensured for us that the faces of the cube were along the [100] direction.

Scanning-electron-microscope (SEM) pictures of the three samples revealed that samples 1 and 2 had similar characteristics. They both had a surface roughness on the order of 0.5 μm. A large number of spherical particles of a diameter on the order of 3 μm were scattered across their surface. The surfaces of sample 1 are shown in Fig. 1, and similar results were obtained from sample

TABLE I. Characteristics of the three UBe_{13} single crystals studied in this work. All samples were annealed for six months at 1000 °C.

Samples	Mass (mg)	Dimensions (mm)	% of Al flux (by molar volume)	Growth cooling rate	T_c ($B_{dc}=0$) (onset)
1	13.55	2.4×1.65×1.0	92%	2.5 °C/h 1200–900 °C	903.5 mK ±0.5 mK
2	5.89	1.65×1.3×1.0	92%	2.5 °C/h 1200–900 °C	901.5 mK ±0.5 mK
3	18.83	2.5×1.9×1.65	90%	5 °C/h 1400–900 °C	849.3 mK ±0.5 mK

2.[28] Possessing grainlike particles ranging from 1 to 50 μm in size, the surface of sample 3, shown in Fig. 2, looked much rougher relative to the surfaces of samples 1 and 2. Prior to taking the SEM pictures, the samples were washed in acetone and reagent alcohol in order to remove any dust, grease, or varnish from the surface. A small area of the surface of sample No. 3 was polished with very fine paper of 0.5 μm grading, and the resultant finish is shown in Fig. 3. We emphasize that all the results presented in this paper are for the unpolished specimen. Figure 3 indicates that the surface defects, observed prior to polishing, do not apparently penetrate into the bulk of the sample. We also performed electron probe microanalysis, with a JEOL Superprobe 733, on samples 2 and 3 to look for the presence of Al and Na. This analysis, for which the sensitivity level was less than 0.5%, did not reveal any traces of these two elements for either sample.

III. RESULTS

This section is divided into three parts. First, the results on the normal-state susceptibility (4 K $< T <$ 17 K) are presented. As mentioned before, these measurements were performed in order to identify which sample, if any, possessed an anomaly around 8 K. Next, our measurements of $B_{c2}(T)$ are presented, with an emphasis on the $T/T_c \rightarrow 1$ limit. The last subsection concentrates on the zero-field temperature dependence of the penetration depth obtained for two of our samples (1 and 3).

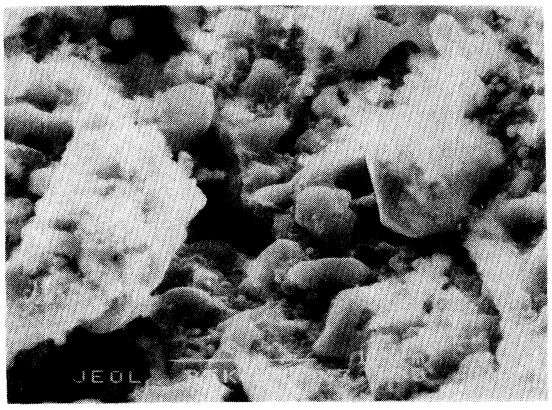

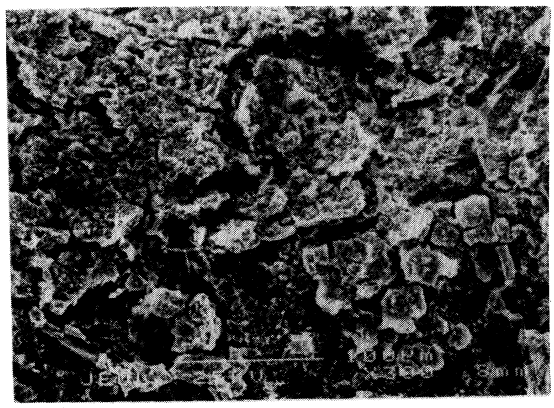

FIG. 2. SEM pictures of the surface of sample 3: (top) 100-μm scale and (bottom) 10-μm scale. With grainlike particles ranging from 1 to 50 μm in size, the surface looks much rougher relative to the surfaces of samples 1 (Fig. 1) and 2 (Ref. 28).

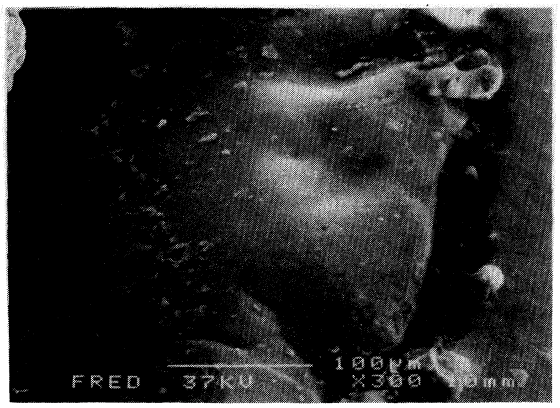

FIG. 3. SEM pictures of the surface of sample 3 after polishing (see text for details): (top) 100-μm scale and (bottom) 10-μm scale. Evidently, the surface defects seen in Fig. 2 do not penetrate into the bulk of the sample.

A. Normal-state results

The magnetic susceptibility in the normal state (4 K $< T <$ 17 K) was measured with a Quantum Design superconducting quantum interference device (SQUID) magnetometer using an applied field of 0.5 T. We note that several UBe_{13} single crystals (in addition to the ones presented here) were studied, and none showed any sign of an anomaly in their susceptibility in the temperature range covered. The results for samples 1 and 3 are shown in Figs. 4 and 5. The data obtained on sample 2 are quite similar to those of sample 3 and are reported in detail elsewhere.[28] At first glance, none of the samples exhibit any strong anomaly within the temperature range swept. However, after ploting (in the insets) the derivative, $d\chi/dT$, samples 2 and 3 (Fig. 5) appear to possess a small

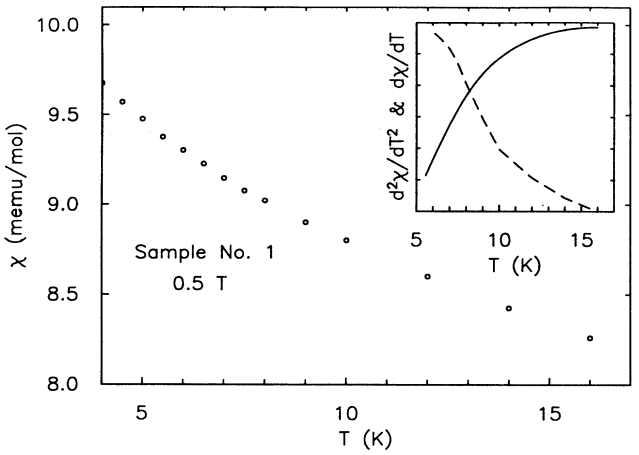

FIG. 4. $\chi(T)$ of samle 1 in the normal state in an applied field of 0.5 T. The inset shows the first (solid line) and second (broken line) derivative of $\chi(T)$ with respect to T. All three curves are smooth, indicating that any potential magnetic transition, if it exists, is not detectable in this temperature range.

kink around 13 K and 12 K, respectively. The second derivative, $d^2\chi/dT^2$, also shown in the insets, helps to emphasize the presence of these subtle features. For sample No. 1, all three curves $[\chi(T), d\chi/dT, d^2\chi/dT^2]$ are smooth through the important temperature region (Fig. 4). Therefore, a comparison of the superconducting properties between sample 1 and samples 2 and 3 might allow us to extract information about the role, if any, played by the normal-state anomaly of the superconducting state of UBe_{13}. In addition, the broad peaks observed around 8 K in the second derivatives for samples 2 and 3 (Fig. 5) represent the natural trend of the susceptibility as

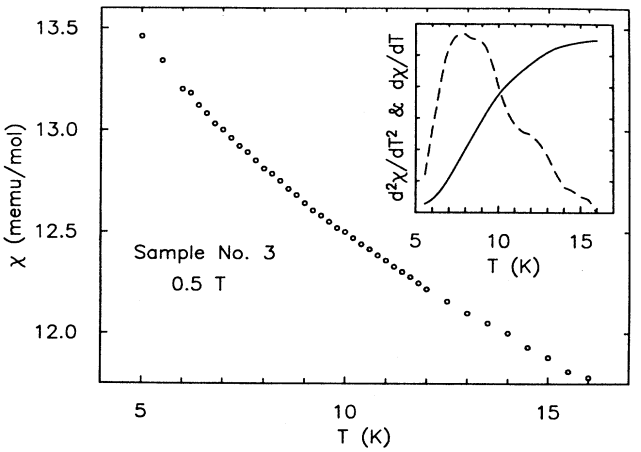

FIG. 5. $\chi(T)$ of sample 3 in the normal state in an applied field of 0.5 T. The inset shows the first (solid line) and second (broken line) derivative of $\chi(T)$ with respect to T. The second derivative curve indicates a large bump around 8 K associated with the leveling of $\chi(T)$ at lower temperatures, and a small anomaly around 12 K.

it leads up to the transition at T_c. The onset of this peak is also seen for sample 1 around 6 K (Fig. 4).

We note that these derivatives represent the slopes of a spline fit, which was allowed to deviate from the data points by a value that corresponds to the scatter in the data. Therefore, the kinks observed in these curves are statistically significant. However, it is important to stress that these anomalies are rather small, barely above the sensitivity of the measurements. The anomalies observed by Aliev *et al.*[22] were much more pronounced, although the comparison is not straightforward, since they measured the thermal conductivity and resistivity. The lack of a pronounced anomaly in the normal state does *not* reflect a poor quality in our samples; on the contrary, samples that are considered of the highest quality do not exhibit any anomalous transition, even using high-sensitivity measuring techniques.[24,25]

B. Phase diagrams

In this subsection, the phase diagrams constructed from our inductive measurements are presented. An important aspect in constructing a phase diagram is the manner in which the values of $B_{c2}(T)$ were determined. The first part of this subsection addresses this point. In the second part, the phase diagrams are presented, followed by the data obtained from magnetic field sweeps.

1. *Determination of* $B_{c2}(T)$

The values of $B_{c2}(T)$ were determined by sweeping the temperature and keeping the magnetic field B_{dc} constant by placing the superconducting magnet into its persistent mode. We therefore identify $B_{c2}(T)$ at a point T_c (B_{dc}=const). For each temperature sweep at constant field, the sample was first cooled to a suitably low temperature (typically 50 mK) in the earth's magnetic field. After the dc field was then slowly ramped up to its set point without significant warming of the specimen, the temperature was slowly increased above $T_c(B)$ at a rate of 10 mK/h. We define T_c as the temperature where the diamagnetic signal changed from its temperature-dependent behavior in the superconducting state to its normal-state value. In other words, we first fit the normal-state data to a straight line and then looked for the first deviation of the data from the fit. This procedure allowed us to locate the temperature at which the last remnant of bulk superconductivity vanished. Two examples of traces used in the determination of $T_c(B)$ for sample 1 and for fields parallel to the [100] direction are shown in Fig. 6. A complete set of data has been compiled elsewhere.[28]

Another important experimental aspect is the manner in which we achieved the two orientations of the specimens with respect to the dc magnetic field. The crystals were oriented with respect to the field before each run. Our technique required that, between runs, the varnish, holding the sample to the copper wires (used for thermal anchoring), be removed. The samples were then rotated, and varnished back onto the copper wires. To ensure

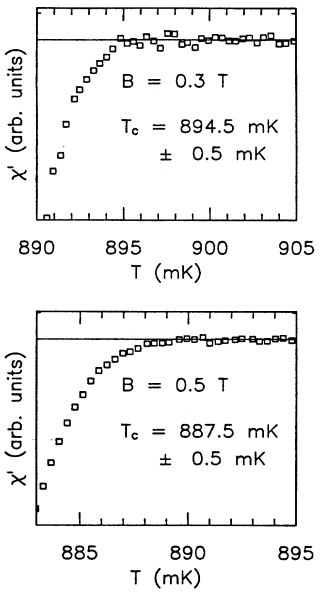

FIG. 6. Determination of $T_c(B)$ for sample 1 with $\mathbf{B}_{dc}\|[100]$ and with $B_{dc}=0.3$ T (top) and $B_{dc}=0.5$ T (bottom). The transition temperature is defined as the first deviation of the data from the normal-state value of $\chi'(T)$.

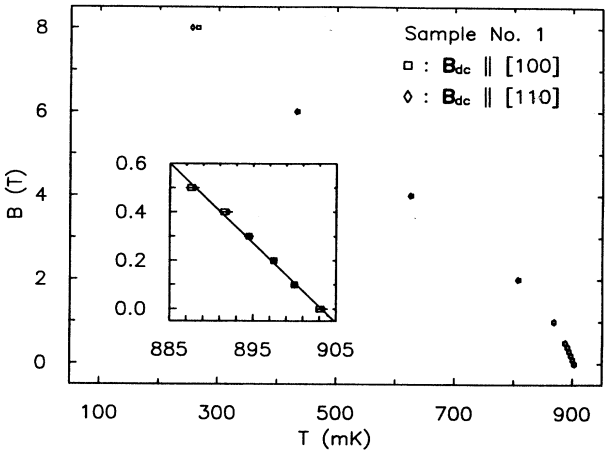

FIG. 7. The B-T phase diagram for sample No. 1 with $\mathbf{B}_{dc}\|[100]$ direction (□) and $\mathbf{B}_{dc}\|[110]$ direction (◊). The inset focuses on the data in the limit $T/T_c\rightarrow 1$. The solid line is the result of a linear fit which indicates that the data fall on a straight line of slope $dB_{c2}(T)/dT=(-32.8\pm0.5)$ T/K.

that we could reproduce the thermal anchoring of the sample from run to run, we used the same crystal orientation ([100)] twice, after dismounting, for one of the specimens (sample 1). The transition temperature of 903 mK was reproducible to within the experimental errors of 0.5 mK.[28] This result indicates that our mounting technique does not introduce additional uncertainties in the identification of T_c.

2. Phase diagrams

The values of $B_{c2}(T)$, obtained from the method described above, allow us to construct the B-T phase diagrams. The resultant diagrams for samples 1 and 3 are shown in Figs. 7 and 8. The phase diagram for sample 2 (see Ref. 28 for detailed data plots) is quite similar to the ones obtained for sample 1 (Fig. 7), and the important differences between the two specimens is listed in Tables I and II. The common feature among the three samples is the lack of anisotropy in the limit $T/T_c\rightarrow 1$, as can be seen in the insets of the figures. This finding, central to our study, will be discussed in detail in the next section.

Another interesting result is the fact that sample 3, which posesses the lowest zero field T_c of 849 mK (compared to 903 and 900 mK for samples 1 and 2; see Table I), exhibits the highest slope, $dB_{c2}(T)/dT\approx -34.5$ T/K at T_c, while the slopes for samples 1 and 2 were -32.8 T/K and -25.5 T/K; see Table II. The combination of a low T_c and a high-$B_{c2}(T)$ slope near $T/T_c\approx 1$ is characteristic of type-II superconductors with impurities, which decrease T_c and increase the upper critical field. This effect has been observed in BCS superconductors such as niobium.[30]

In order to further the comparison between the samples, we report the superconducting transition width W, defined as the temperature interval between 10% and 90% of the total transition. For samples 1 and 2, $W=70\pm10$ mK in zero field and $W=160\pm10$ mK in a 1-T field, while, for sample 3, $W=100\pm10$ mK in zero field and $W=160\pm10$ mK in a 1-T field.

3. $\chi'(B)$ at constant temperatures

In addition to our temperature sweeps at constant magnetic fields, we performed a series of magnetic-field sweeps at constant temperature. The initial motivation

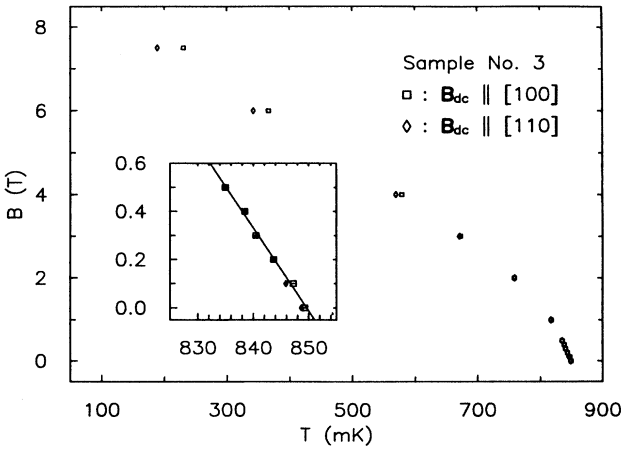

FIG. 8. The B-T phase diagram for sample 3 with $\mathbf{B}_{dc}\|[100]$ direction (□) and $\mathbf{B}_{dc}\|[110]$ direction (◊). The inset focuses on the data in the limit $T/T_c\rightarrow 1$. The solid line is the result of a linear fit which indicates that the data fall on a straight line of slope $dB_{c2}(T)/dT=(-34.5\pm0.5)$ T/K.

TABLE II. Summary of results obtained on the three single crystals of UBe_{13}.

Samples	$\chi'(T)$ subtle feature in normal state	λ $(T/T_c \leq 0.5)$	Anisotropy for $T/T_c \rightarrow 1$	dB_{c2}/dT for $T/T_c \rightarrow 1$	$\Delta T_c(B)$ $(T_c[100]-T_c[110])$
1	No	$\sim T^{2.8\pm0.2}$	No	-32.8 ± 0.5 T/K	5±1 mK, $B_{dc}=8$ T
2	Yes, near 13 K	No data taken	No	-25.5 ± 1.0 T/K	40±5 mK, $B_{dc}=8$ T
3	Yes, near 12 K	$\sim T^{2.6\pm0.2}$	No	-34.5 ± 0.5 T/K	40±5 mK, $B_{dc}=7.5$ T

for this measurement came from the report by Ellman *et al.*[27] of a second transition line, within the superconducting state, observed by measuring the specific heat as a function of field at constant temperature. The transition line reported by Ellman *et al.* was nearly constant in field (i.e., approximately parallel to the temperature axis in a B-vs-T plot) and was, therefore, difficult to observe from temperature sweeps. If the feature observed by Ellman *et al.* corresponds to a new phase, we would expect our measurements to show a shoulderlike signal in $\chi'(B,T)$ and a peak in $\chi''(B,T)$, as observed in UPt_3.[28,31] Our results obtained for samples 1 are shown in Fig. 9, where there is no obvious presence of any second transition below $B_{c2}(T)$. Similar results have been obtained in sample 2.[28] However, both samples exhibit a double bump in $\chi''(B)$ near $B_{c2}(T_c)$, which corresponds to a kink in $\chi'(B)$. This observation is probably related to the fact that, due to the parallelepiped shape of the samples, the field is not homogeneously distributed around the surface. Consequently, parts of the specimen (edges and corners) experience fields greater than $B_{c2}(T)$ and become normal, while the rest of the sample stays superconducting. The coexistence of normal and superconducting volumes within a given sample is known as the intermediate state. A similar behavior for $\chi'(B)$ has been observed in niobium[30] and was also accounted for by the intermediate state. We note that, since our criterion for T_c is the onset of superconductivity, this effect does *not* affect the determination of T_c and the phase diagrams (Figs. 7 and 8).

Magnetic field sweeps on sample No. 3 revealed a different and interesting feature in $\chi'(B)$. Three sweeps, for fields parallel to the [100] direction and performed at 100, 175, and 250 mK, indicated a bump in $\chi'(B)$ just below the upper critical field transitions,[28] and the 250 mK sweeps for both orientations are shown in Fig. 10 as an example. This effect is different from the one discussed in the preceding paragraph, since, for sample 3, $\chi'(B)$ goes through a local maximum, which cannot be explained in terms of the intermediate state. The inset of Fig. 10 focuses on the magnetic-field range for which these bumps occurred. In order to map out the B-T diagram of this feature, the peak of the bump, labeled B^* and indicated in the inset, was identified for our various sweeps. For the high-temperature/low-field region, we

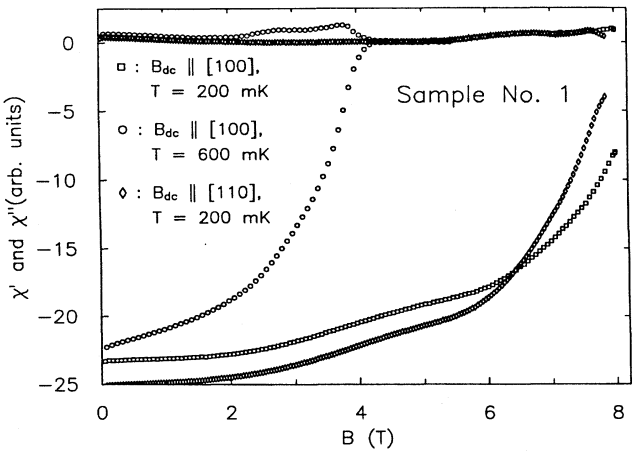

FIG. 9. $\chi'(B)$ and $\chi''(B)$ (zero-field cooling conditions) for sample 1 for the applied dc field, $\mathbf{B}_{dc}$, parallel to the [100] direction and at constant temperature $T=200$ mK (□); $\mathbf{B}_{dc}\|[100]$, $T=600$ mK (○); and $\mathbf{B}_{dc}\|[110]$, $T=200$ mK (◊). For the 200-mK sweeps, $B_{c2}(200\text{ mK})$ is greater than 8 T.

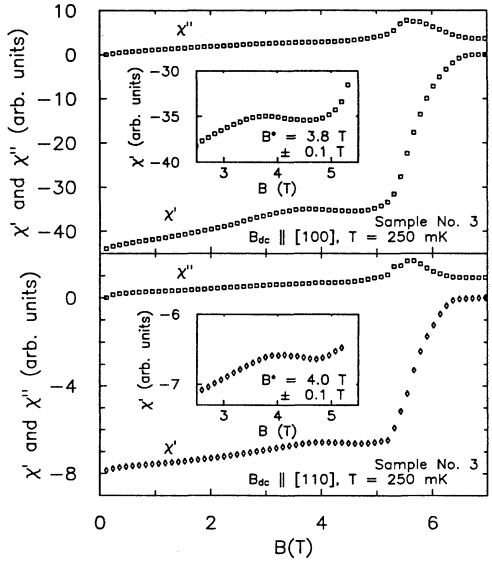

FIG. 10. $\chi'(B)$ and $\chi''(B)$ (zero-field-cooling conditions) for sample 3 with (top) $\mathbf{B}_{dc}\|[100]$ and (bottom) $\mathbf{B}_{dc}\|[110]$, for $T=250$ mK. The insets show the feature in $\chi'(B)$ around $B^*=3.8$ T (top), and $B^*=4.0$ T (bottom).

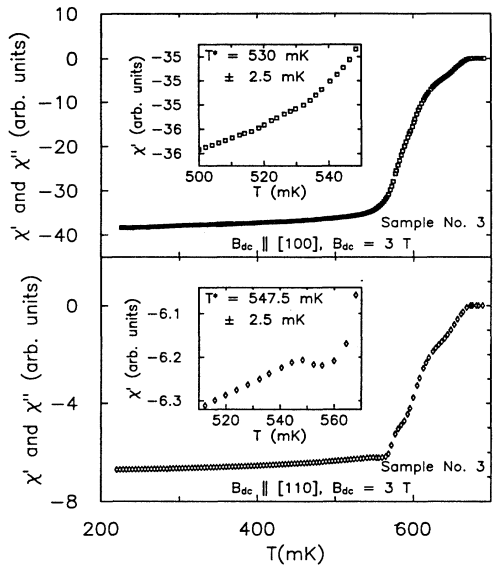

FIG. 11. $\chi'(T)$ (zero-field-cooling conditions) for sample 3 with $B_{dc}=3$ T, $\mathbf{B}_{dc}\|[100]$ (top), $\mathbf{B}_{dc}\|[100]$ (bottom). The insets show the anomaly in $\chi'(T)$ around $T^*=530$ mK (top) and $T^*=547.5$ mK (bottom).

switched to temperature sweeps at constant field, and typical data are shown in Fig. 11 for $B_{dc}=3$ T for both orientations. From these types of traces, we extracted T^*, the temperature at which the bump occurs. We note that T^* was clearly observable for the fields parallel to the [110] direction, even down to $B_{dc}=0$, while the bump was not as well defined for fields parallel to the [100] direction. The phase diagram constructed from these values of B^* and T^* is shown in Fig. 12, where the upper critical field is also plotted for comparison. In the

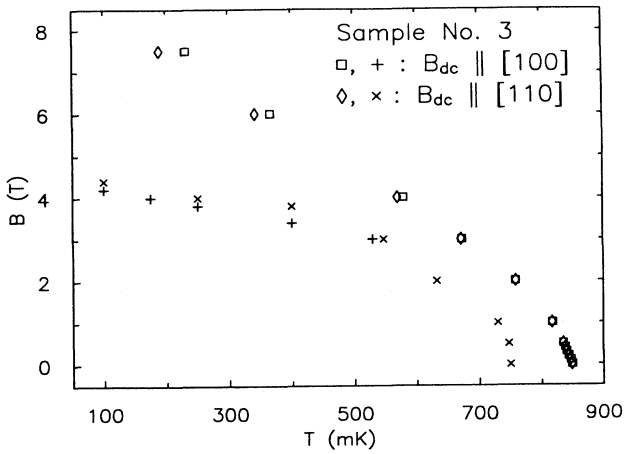

FIG. 12. The B-T phase diagram for sample 3 with $\mathbf{B}_{dc}\|[100]$ ($\square,+$) and $\mathbf{B}_{dc}\|[110]$($\Diamond,\times$). The crosses and multiplication signs correspond to (1) the maxima of the bumps observed in the field sweeps (B^*) and (2) the maxima of the bumps observed in the temperature sweeps (T^*). Also shown, is the upper critical field of sample 3 for $\mathbf{B}_{dc}\|[100]$ ($\square$) and $\mathbf{B}_{dc}\|[110]$($\Diamond$). The error bars are less than the size of the symbols.

next section, the nature of this anomaly is argued to be related to flux-line depinning and to be an extrinsic feature of the superconductivity in UBe_{13}.

C. Zero-field-temperature dependence of $\lambda(T)$

The temperature dependence of the penetration depth $\lambda(T)$ was obtained with a mutual inductance technique identical to the one described in our previous work,[28,31] where we showed that

$$\lambda(T)\propto\chi'(T) \quad \text{when } \chi''(T)=0 \; . \tag{1}$$

We studied $\lambda(T)$ of sample No. 1 with the probing ac magnetic field parallel to the [100] and [110] orientations. These results are shown in Figs. 13 through 16. We also measured $\lambda(T)$ of sample No. 3 for the ac field parallel to the [100] orientation, and the data are shown in Figs. 17 and 18.

Figures 13, 15, and 17 show $\chi'(T)$ and $\chi''(T)$ for the entire temperature range studied, while Figs. 14, 16, and 18 show the data for $T/T_c\leq 0.6$. For these low-temperature traces, the data for the reactive response $[\chi'(T)]$ is fitted to $\lambda(T)$, given by the weak coupling BCS theory.[28] As mentioned above, $\chi'(T)$ is directly proportional to $\lambda(T)$ as long as $\chi''(T)=0$, which is true for $T/T_c\leq 0.6$, justifying our analysis. We note that the results of the fits are insensitive to the value of the specific-heat jump at the transition temperature $(\Delta C/C_N)|_{T_c}$, for $1\leq(\Delta C/C_N)|_{T_c}\leq 2$.

The insets of Figs. 14, 16, and 18 show log-log plots of the data. Linear fits indicate that the temperature dependences of samples 1 (both orientations) and 3 are close to T^η, $2.5<\eta<3$. This result is not surprising, since the exponential temperature dependence predicted by the BCS theory is very close to T^3 for $T/T_c>0.1$.[5] A cubic temperature dependence in the $T\rightarrow 0$ limit is also consistent with the presence of line nodes in the energy gap structure.[5] However, within this interpretation, some anisot-

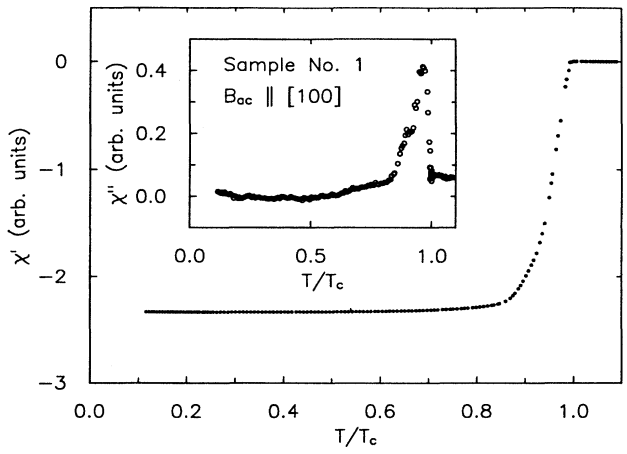

FIG. 13. $\chi'(T)$ and $\chi''(T)$ (inset) for sample 1 with the probing field parallel to the [100] direction.

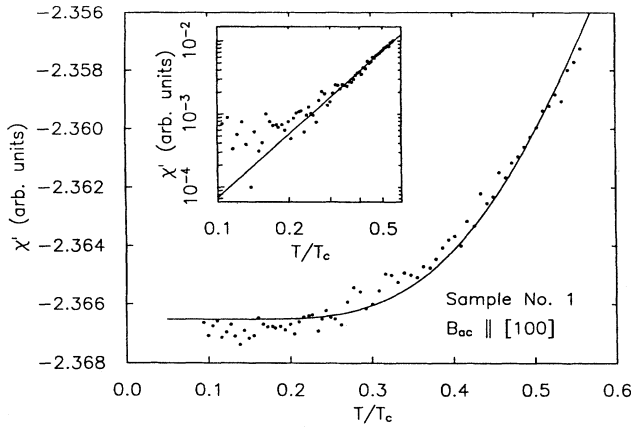

FIG. 14. $\chi'(T)$ for sample 1 with the probing field parallel to the [100] direction and for $T/T_c < 0.6$. The line corresponds to a fit to the BCS weak-coupling theory. The inset shows a log-log plot. The linear fit indicates that the data fall on a straight line of slope 2.9 ± 0.5.

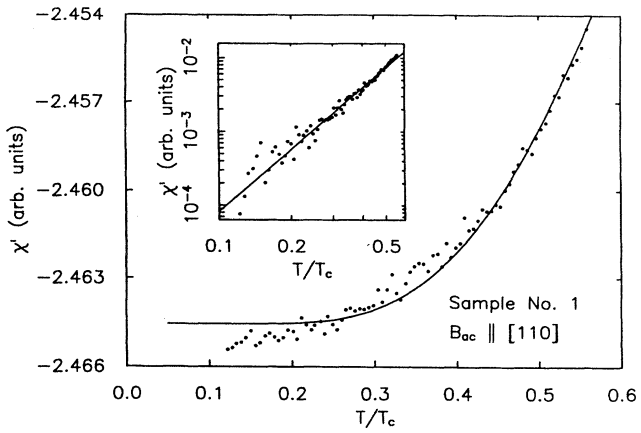

FIG. 16. $\chi'(T)$ for sample 1 with the probing field parallel to the [110] direction and for $T/T_c < 0.6$. The line corresponds to a fit to the BCS weak-coupling theory. The inset shows a log-log plot. The linear fit indicates the data fall on a straight line of slope 2.8 ± 0.2.

ropy is expected, in contrast to the T^{η}, $\eta \approx 3$ dependence observed for sample 1, for the probing ac magnetic field parallel to the [100] and [110] directions. Therefore, our results on the temperature dependence of $\lambda(T)$ do not determine whether UBe_{13} is a conventional or an unconventional superconductor.

IV. DISCUSSION

In this section, the main results presented above and summarized in Table II are discussed. First, the isotropic results on $B_{c2}(T)$ in the limit $T/T_c \rightarrow 1$ (Figs. 7 and 8) are discussed, along with arguments explaining the discrepancy between these results and those reported by Aliev *et al.*[22] Second, the anomaly, below $B_{c2}(T)$, observed for sample 3 (Figs. 10–12) is analyzed. Third, the temperature dependence of $\lambda(T)$ obtained from our $\chi'(T)$ in zero field is considered.

A. Anisotropy in $B_{c2}(T)$ in the limit $T/T_c \rightarrow 1$

An important result from our measurements is the fact that, within our experimental uncertainties, the upper critical field is isotropic in the limit $T/T_c \rightarrow 1$. As mentioned earlier, Gor'kov has discussed the presence of anisotropy in $B_{c2}(T)$ in the low-field regime for unconventional superconductors.[13] Our results do not, however, rule out unconventional superconductivity in UBe_{13}. First, it is possible that the anisotropy exists, but cannot be observed with our experimental sensitivity. For instance, if the anisotropy is less than 0.5 mK at 0.5 T, our

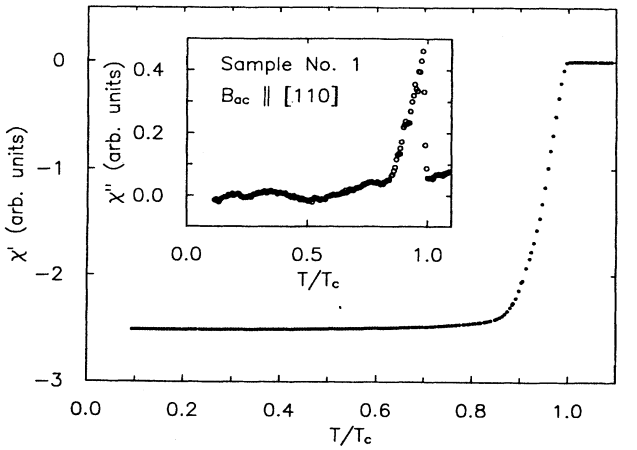

FIG. 15. $\chi'(T)$ and $\chi''(T)$ (inset) for sample 1 with the probing field parallel to the [110] direction.

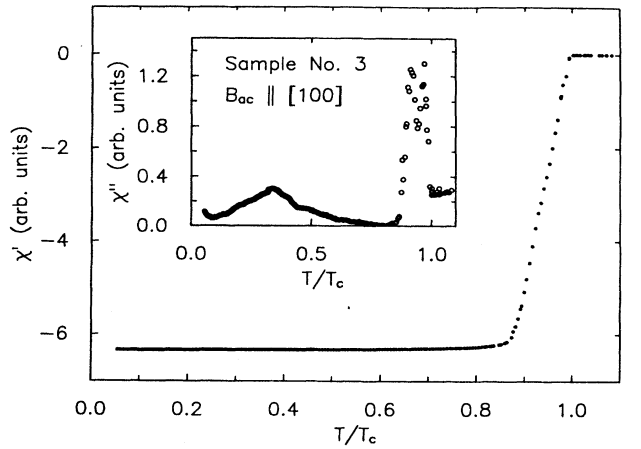

FIG. 17. $\chi'(T)$ and $\chi''(T)$ (inset) for sample 3 with the probing field parallel to the [100] direction.

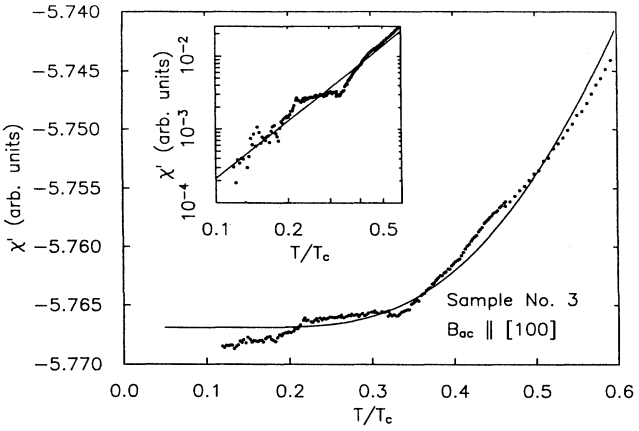

FIG. 18. $\chi'(T)$ for sample 3 with the probing field parallel to the [100] direction and for $T/T_c < 0.6$. The line corresponds to a fit to the BCS weak-coupling theory. The inset shows a log-log plot. The linear fit indicates the data fall on a straight line of slope 2.6 ± 0.2.

measurements would not detect it. Second, more unconventional superconducting states may give an isotropic $B_{c2}(T)$.[32]

From the values of the slope of $B_{c2}(T)$ in the limit $T/T_c \rightarrow 1$, and following the procedure outlined by Maple *et al.*,[15] for weak-coupling superconductors in the dirty limit, one can estimate the coherence length ξ of UBe_{13}. Using the value of $dB_{c2}(T)/dT = -32.8 \pm 0.5$ T/K found for sample 1, we estimate $\xi \approx 156 \pm 5$ Å. From the slopes of $B_{c2}(T)$ for sample 2 (-25.5 ± 0.5 T/K) and sample 3 (-34.5 ± 0.5 T/K), we estimate $\xi \approx 227 \pm 5$ Å and $\xi \approx 148 \pm 5$ Å, respectively. These values are in agreement with the one reported by Maple *et al.*[15] (142 Å), with the exception of the result from sample 2.

We now discuss the discrepancy between our results [isotropic $B_{c2}(T)$ in the limit $T/T_c \rightarrow 1$] and the ones reported by Aliev *et al.*[22] There exist several possible explanations for this discrepancy. First, our samples were annealed, while the specimens that Aliev *et al.* measured were not. It is possible that an anisotropic distribution of impurities give rise to an anisotropic $B_{c2}(T)$. This assertion could be checked by annealing the crystals studied by Aliev *et al.* and remeasuring the upper critical field.

A second possible explanation is related to the well-known phenomenon of flux-flow resistance in type-II superconductors.[33] As a current **I** (this is the current used to measure resistivity) flows through a type-II superconductor placed in a magnetic field, B_{dc} ($B_{dc} > B_{c1}$), the flux lines experience a Lorentz force

$$\mathbf{F} = \mathbf{I} \times \frac{1}{c} \mathbf{B}_{dc} , \tag{2}$$

where c is the speed of light. Due to this force, the flux lines will tend to move transverse to the currents. This flux flow occurs if the thermal energy overcomes the pinning energy of the vortices. As the flux lines move across the sample with velocity **v**, they induce an electric field parallel to **I**, given by

$$\mathbf{E} = \mathbf{B} \times \frac{\mathbf{v}}{c} , \tag{3}$$

which acts like a resistive voltage. In type-II superconductors, because the pinning energy is rather low, flux-flow resistance is observable even at temperatures significantly below the critical temperature. This effect is of particular importance in high-temperature superconductors. In fact, Tinkham[34] showed how the shape of the resistive transitions in these materials depend on the strength of the pinning energy relative to thermal energy. It is clear that anisotropy in the pinning energy of the vortices will cause an anisotropy in the shapes of the resistive transitions. Such pinning energy anisotropy is likely to be present in single crystals, where dislocation and microcracks are more likely to form along specific crystal directions. If the shape of the resistive transition changes with the orientation of the field, then the $T_c(B)$ determined by the midpoint of the resistive transitions are likely to reflect the anisotropy of the pinning energy. For this reason, it is preferable to determine $T_c(B)$ as the *onset* of the resistive transition.

The third possible explanation for understanding the anisotropic results of Aliev *et al.* is related to the demagnetization factor, and (again) to the fact that the midpoint of the transition was chosen to identify $T_c(B)$. The demagnetization factor D is a property of a magnetic sample, depending on the shape of the specimen, and the orientation of the magnetic field relative to it. In what follows, we have to differentiate between the magnetic field strength H (in A/m) and the magnetic field induction, B (in T) related by $B = \mu H$, where μ is the magnetic permeability of the material. The demagnetization factor can be expressed in terms of the applied field strength H_0, the field strength inside the sample (or the field strength that the sample experiences as a whole) H_i, and the magnetization of the sample M by the expression

$$H_i = H_0 - DM . \tag{4}$$

The magnetization of the sample M is related to H_i and B_i (the magnetic induction inside the sample) by the usual relation

$$M = \frac{1}{\mu} B_i - H_i . \tag{5}$$

We know that for a superconductor exhibiting a perfect Meissner effect $B_i \approx 0$, so that Eq. (4) becomes

$$H = \frac{H_0}{(1-D)} . \tag{6}$$

Equation (6) indicates that, if the demagnetization factor of a superconducting sample is nonzero ($D = 0$ corresponds to an infinite cylinder in a longitudinal field), then the magnetic-field strength that the sample experiences is greater than the applied field strength. Consequently, if one ignores the demagnetization effect, while measuring the critical field of a superconductor, one underestimates

the true value of $B_{c2}(T)$. Furthermore, since D depends on the orientation of the applied field with respect to the sample, measuring $B_{c2}(T)$, while ignoring the effects of D, will yield an anisotropic $B_{c2}(T)$. However, it is important to keep in mind that this effect is present for a sample exhibiting a complete Meissner effect. For a type-II superconductor, in fields above B_{c1}, a complete Meissner effect is not fully achieved. In fact, M drops to zero at the onset of the transition, so that the demagnetization factor does not play a role in *our* measurements, and the field experienced by the sample is equal to the applied field. Again, we see the importance of using the onset of the transition as the criterion for $T_c(B)$. On the other hand, at the midpoint of the transition [used by Aliev *et al.* as their criterion for $T_c(B)$] M is finite, and the demagnetization effect introduces an anisotropy in $B_{c2}(T)$ if it is ignored in the analyses of the data. It is possible that data of Aliev *et al.* reflect the anisotropy of the demagnetization factor of their sample.

B. Anomaly in sample 3

The phase diagram for sample 3 presented in Fig. 12 indicates the presence of a second transition line within the superconducting state. This second transition line was constructed by following the dependence of an anomaly in $\chi'(B)$ and $\chi'(T)$ as a function of temperature and field (Figs. 10 and 11). In addition, a comparison of our measurements for fields parallel to the [100] orientation with the data for fields parallel to the [110] orientation suggests that the anomaly is more pronounced in the latter measurements.[28] We now argue that this anomaly is related to a change in the flux-line distribution inside the sample and that it is caused by a large amount of pinning sites present in sample 3.

The assertion that flux-line pinning plays an important role in sample 3 is supported by the fact that this specimen features a reduced transition temperature, along with an enhanced slope of $B_{c2}(T)$ near T_c. This combination is characteristic of type-II superconductors possessing numerous pinning sites. The argument is further supported by the SEM pictures of the surface of sample 3 (Fig. 2), which indicate a large amount of surface roughness that could provide additional pinning sites. More specifically, consider Fig. 10, which shows two typical sweeps of $\chi'(B)$. As the magnetic field is slowly increased above the lower critical field, the flux lines penetrate the sample but initially get pinned near the surface, thereby blocking the entrance of additional flux lines inside the bulk of the sample. As the field is further increased, the flux-line density at the surface exceeds $B_{c2}(T)$ locally, and it becomes energetically favorable for the flux lines to occupy a lattice throughout the bulk of the sample. In Fig. 10, this rearrangement of flux lines takes place around 3.8 T and 4.0 T for $\mathbf{B}_{dc}\|[100]$ and $\mathbf{B}_{dc}\|[110]$, respectively. As the applied field is further increased and approaches $B_{c2}(T)$, more flux lines penetrate the sample, and the transition to the normal state occurs.

Recently, thermal expansion measurements by van Dijk *et al.* have suggested the presence of a similar flux distribution transition in URu_2Si_2.[35] These authors reported a change in sign of the hysteresis loop occurring below $B_{c2}(T)$. The sign observed at low temperatures and low fields corresponds to flux pinning effects, while the sign for higher field and higher temperature is not clearly understood, although it is most likely related to a change in the flux-line distribution. Van Dijk *et al.* also reported most anisotropy associated with their measurements, consistent with our own results, which showed that the effect was more pronounced for $\mathbf{B}_{dc}\|[110]$ than for $\mathbf{B}_{dc}\|[100]$. Within the interpretation given in the preceding paragraph, this anisotropy can be understood by the fact that the cross-section area of the sample oriented with $\mathbf{B}_{dc}\|[110]$ is larger than that for $\mathbf{B}_{dc}\|[100]$, so that more pinning sites are available and the effect is amplified. Similar changes of sign in the hysteresis loop have also been reported for UBe_{13} samples studied by de Visser *et al.*[24]

C. Temperature dependence of $\lambda(T)$

Our data of $\chi'(T)$ in zero field (Figs. 14, 16, and 18) suggest that the penetration depth in UBe_{13} follows a power law close to T^3. Because the exponential temperature dependence predicted from the weak-coupling BCS is very close to a T^3 dependence,[5] the case for unconventional superconductivity cannot be made for UBe_{13} on the basis of these measurements alone. It is interesting to note that our results disagree with previous penetration-depth measurements that indicated a T^2 temperature dependence of $\lambda(T)$.[5] Gross-Alltag *et al.*[6] suggested that their quadratic temperature dependence could be the signature of either a gap having point nodes (axial state) or the presence of impurities in the sample. According to their calculations, a T^3 temperature dependence of $\lambda(T)$ suggests an energy gap with lines of nodes on the Fermi surface. Furthermore, Ramirez *et al.*,[36] based on their specific-heat measurements as a function of field, have argued for the existence of lines of nodes in UBe_{13}. However, within this interpretation, different temperature dependences are expected for different orientations of the magnetic field with respect to the lines of nodes, and, therefore, our T^η, $\eta \approx 3$, results for both $\mathbf{B}_{dc}\|[100]$ and $\mathbf{B}_{dc}\|[110]$ are difficult to reconcile with the presence of line nodes. Since our measurements have not been performed in the very-low-temperature limit ($T/T_c < 0.1$), the temperature dependence we observed may not be the true $T \rightarrow 0$ temperature dependence.

V. SUMMARY

First, our measurements of the upper critical field indicate that, within our experimental uncertainties of 0.5 mK and 0.5 mT, $B_{c2}(T)$ is isotropic in the limit $T/T_c \rightarrow 1$. Arguments were given to explain the discrepancy between our results and the ones reported by Aliev *et al.*[22] In particular, we showed that their criterion of $T_c(B)$ as the midpoint of the resistive transition could introduce some anisotropy in their results, and that using the onset of the transition, as we did, is a better criterion. Consequently, although our results provide constraints on the underlying symmetry of the superconduct-

ing order parameter in UBe_{13}, they do not elucidate details about the microscopic picture.

Secondly, we did not observe any signs of second transition within the superconducting state in our highest-quality samples (1 and 2). Sample 3 exhibited an anomaly below B_{c2} (T), and we argued that it was not intrinsic to UBe_{13} but related to flux-pinning mechanisms, which are expected to play an important role in the mixed state of type-II superconductors possessing large numbers of pinning sites.

Finally, the temperature dependence of the penetration depth for $0.1 \leq T/T_c \leq 0.5$ was found to be close to T^3 for both $\mathbf{B}_{dc} \| [110]$ and $\mathbf{B}_{dc} \| [100]$. To date, there exists no theoretical work that can explain these results in terms of a superconducting state with an energy gap possessing nodes. On the other hand, because the temperature dependence expected for a BCS superconductor is also close to T^3 for $T/T_c > 0.1$, these measurements, alone, cannot be taken as evidence for unconventional superconductivity.

ACKNOWLEDGMENTS

Throughout the course of this work, we have benefited from enlightening conversations and correspondence with many colleagues, including A. de Visser, P. J. Hirschfeld, J. A. Sauls, F. Sharifi (who also kindly provided us with the use of his scanning electron microscope), and S. K. Yip. We are grateful to A. P. Ramirez and J. L. Smith for communicating Ref. 36 to us prior to publication. Several aspects of this work have used the facilities of the UF Major Analytical Instrumentation Center (MAIC). This work was supported, in part, by the National Science Foundation (Grant Nos. DMR-9200671 for P.J.C.S. and M.W.M. and DMR-9400755 for B.A.) and the U.S. Department of Energy (Grant No. DE-FG05-86ER45268 for G.R.S.). One of us (M.W.M.) gratefully acknowledges the hospitality of Northwestern University and the NU-MRC UPt_3 Thrust Group during the preparation of this manuscript.

*Also at University of Augsburg, 86159 Augsburg, Germany.
†Electronic address: meisel@phys.ufl.edu

[1]For experimental reviews, see, for example, G. R. Stewart, Rev. Mod. Phys. **56**, 755 (1984); J. L. Smith, Philos. Mag. B **65**, 1367 (1992); Z. Fisk and G. Aeppli, Science **260**, 38 (1993); H. v. Löhneysen, Physica B **197**, 551 (1994).

[2]For theoretical reviews, see, for example, M. Sigrist and K. Ueda, Rev. Mod. Phys. **63**, 239 (1991); R. Joynt, J. Magn. Magn. Mater. **108**, 31 (1992); J. A. Sauls, J. Low Temp. Phys. **95**, 153 (1994); Adv. Phys. **43**, 113 (1994).

[3]H. R. Ott, H. Rudigier, Z. Fisk, and J. L. Smith, Phys. Rev. Lett. **50**, 1595 (1983); H. R. Ott, H. Rudigier, T. M. Rice, K. Ueda, Z. Fisk, and J. L. Smith, *ibid.* **52**, 1915 (1984); N. Grewe and F. Steglish, *Handbook on the Physics and Chemistry of the Rare Earths* (Elsevier Science Publisher, Amsterdam, 1991), Vol. 14.

[4]D. Einzel, P. J. Hirschfeld, F. Gross, B. S. Chandrasekhar, K. Andres, H. R. Ott, J. Beuers, Z. Fisk, and J. L. Smith, Phys. Rev. Lett. **56**, 2513 (1986).

[5]F. Gross, B. S. Chandrasekhar, D. Einzel, K. Andres, P. J. Hirschfeld, H. R. Ott, J. Beuers, Z. Fisk, and J. L. Smith, Z. Phys. B **64**, 175 (1986).

[6]F. Gross-Alltag, B. S. Chandrasekhar, D. Einzel, P. J. Hirschfeld, and K. Andres, Z. Phys. B **82**, 243 (1991).

[7]B. Golding, D. J. Bishop, B. Batlogg, W. H. Haemmerle, Z. Fisk, J. L. Smith, and H. R. Ott, Phys. Rev. Lett. **55**, 2479 (1985).

[8]D. Rainer, Phys. Scr. T **23**, 113 (1987).

[9]P. Fulde, J. Keller, and G. Zwicknagl, in *Solid State Physics*, edited by H. Ehrenreich and D. Turnbull (Academic, San Diego, 1988), Vol. 41.

[10]C. C. Tsuei, J. R. Kirtley, C. C. Chi, Lock See Yu-Jahnes, A. Gupta, T. Shaw, and B. Ketchen, Phys. Rev. Lett. **73**, 593 (1994).

[11]S. K. Yip and J. A. Sauls, Phys. Rev. Lett. **69**, 2264 (1992).

[12]M. Sigrist and T. M. Rice, Europhys. Lett. **3**, 629 (1987).

[13]L. P. Gor'kov, Sov. Sci. Rev. A **9**, 1 (1987).

[14]J. W. Chen, S. E. Lambert, M. B. Maple, M. J. Naughton, J. S. Brooks, Z. Fisk, J. L. Smith, and H. R. Ott, J. Appl. Phys. **57**, 3076 (1985).

[15]M. B. Maple, J. W. Chen, S. E. Lambert, Z. Fisk, J. L. Smith, H. R. Ott, J. S. Brooks, and M. J. Naughton, Phys. Rev. Lett. **54**, 477 (1985).

[16]U. Rauchschwalbe, U. Ahlheim, F. Steglich, D. Rainer, and J. J. M. Franse, Z. Phys. B **60**, 379 (1985).

[17]G. Remenyi, D. Jaccard, J. Flouquet, A. Briggs, Z. Fisk, J. L. Smith, and H. R. Ott, J. Phys. (Paris) **47**, 367 (1986).

[18]G. M. Schmiedeshoff, Y. P. Ma, J. S. Brooks, M. B. Maple, Z. Fisk, and J. L. Smith, Phys. Rev. B **38**, 2934 (1988).

[19]J. P. Brison, J. Flouquet, and G. Deutscher, J. Low Temp. Phys. **76**, 453 (1989).

[20]G. M. Schmiedeshoff, Z. Fisk, and J. L. Smith, Phys. Rev. B **45**, 10 544 (1992).

[21]N. E. Alekseevskii, V. I. Nizhankovskii, V. N. Narozhnyi, E. P. Khlybov, and A. V. Mitin, J. Low Temp. Phys. **64**, 87 (1986).

[22]F. G. Aliev, V. Kovachik, V. V. Moshchalkov, V. V. Pryadun, N. E. Alekseevskii, A. V. Mitin, N. Agrait, S. Vieira, and R. Villar, J. Low Temp. Phys. **85**, 359 (1991).

[23]R. N. Kleiman, D. J. Bishop, H. R. Ott, Z. Fisk, and J. L. Smith, Phys. Rev. Lett. **64**, 1975 (1990).

[24]A. de Visser, N. H. van Dijk, K. Bakker, J. J. M. Franse, A. Lacerda, J. Flouquet, Z. Fisk, and J. L. Smith, Phys. Rev. B **45**, 2962 (1992); J. Magn. Magn. Mater. **108**, 56 (1992).

[25]J. A. Clayhold and H. R. Ott, Bull. Am. Phys. Soc. **38**, 80 (1993).

[26]P. J. C. Signore, B. Andraka, G. R. Stewart, and M. W. Meisel, Physica B **194-196**, 2029 (1994).

[27]B. Ellman, T. F. Rosenbaum, J. S. Kim, and G. R. Stewart, Phys. Rev. B **44**, 12 074 (1991).

[28]P. J. C. Signore, Ph.D. dissertation, University of Florida, Gainesville, 1994. Available from University Microfilms.

[29]M. W. Meisel, G. R. Stewart, and E. D. Adams, Cryogenics **29**, 1168 (1989).

[30]E. S. Rosenblum and S. H. Autler, Rev. Mod. Phys. **36**, 77 (1964).

[31]P. J. C. Signore, B. Andraka, M. W. Meisel, S. E. Brown, Z. Fisk, A. L. Giorgi, J. L. Smith, F. Gross, E. Schuberth, and A. A. Menovsky, Phys. Rev. B **52**, 4446 (1995).
[32]L. I. Burlachkov, Sov. Phys. JETP **62**, 800 (1985).
[33]B. Bertman and M. Strongin, Phys. Rev. **147**, 268 (1966).
[34]M. Tinkham, Phys. Rev. Lett. **61**, 1658 (1988).
[35]N. H. van Dijk, A. de Visser, J. J. M. Franse, and A. A. Menovsky, Physica B **206&207**, 583 (1995).
[36]A. P. Ramirez, C. M. Varma, Z. Fisk, and J. L. Smith (unpublished).

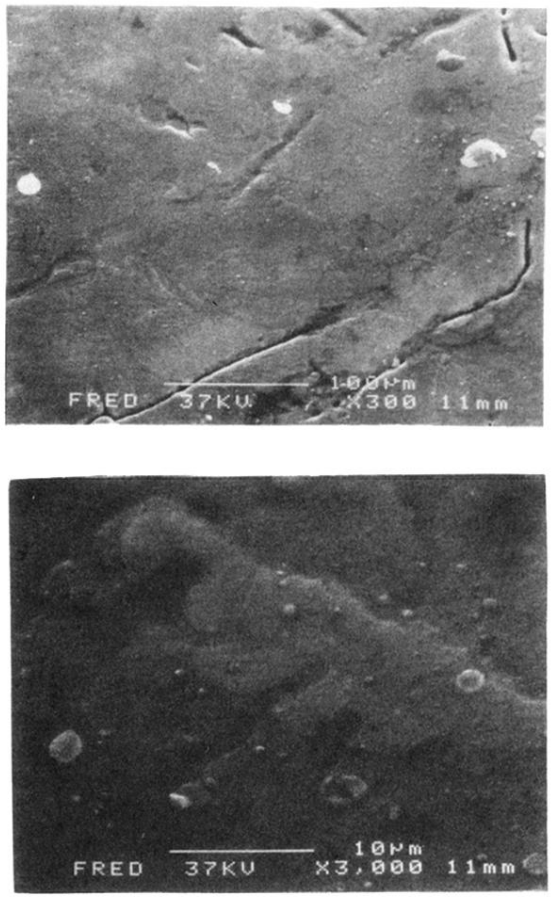

FIG. 1. SEM pictures of the surface of sample 1: (top) 100-μm scale and (bottom) 10-μm scale.

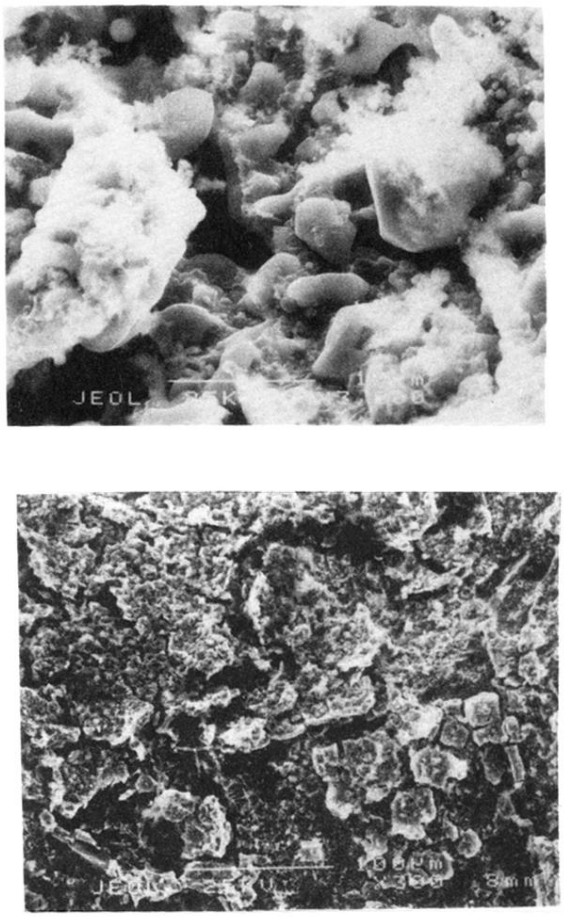

FIG. 2. SEM pictures of the surface of sample 3: (top) 100-μm scale and (bottom) 10-μm scale. With grainlike particles ranging from 1 to 50 μm in size, the surface looks much rougher relative to the surfaces of samples 1 (Fig. 1) and 2 (Ref. 28).

FIG. 3. SEM pictures of the surface of sample 3 after polishing (see text for details): (top) 100-μm scale and (bottom) 10-μm scale. Evidently, the surface defects seen in Fig. 2 do not penetrate into the bulk of the sample.